Improved triangular subdivision schemes[1]

Hartmut Prautzsch[2] Georg Umlauf[3]

Fakultät für Informatik, Universität Karlsruhe,
D-76128 Karlsruhe, Germany
E-mail: [2]prau@ira.uka.de
[3]umlauf@ira.uka.de

Abstract

In this article we improve the butterfly and Loop's algorithm. As a result we obtain subdivision algorithms for triangular nets which can be used to generate G^1- and G^2-surfaces, respectively.

Keywords: Subdivision, interpolatory subdivision, Loop's algorithm, butterfly algorithm.

1. Introduction

Subdivision algorithms are popular in CAGD since they provide simple, efficient tools to generate arbitrary free form surfaces. For example, the algorithms by Catmull and Clark [3] and Loop [7] are generalizations of well-known spline subdivision schemes. Therefore the surfaces produced by these algorithms are piecewise polynomial and at ordinary points curvature continuous.

At extraordinary points however, the curvature is zero or infinite. In general, singularities at extraordinary points is an inherent phenomenon of subdivision, see [13, 12, 9].

The smoothness of a subdivision surface at its extraordinary points depends on the spectral properties of the associated subdivision matrix.

Doo and Sabin [4] derived necessary conditions on the eigenvalues. Ball and Storry [1, 2] made first rigorous investigations to prove the tangent plane continuity for a class of Catmull/Clark type algorithms. Then Reif [11] observed that tangent plane continuous surfaces may have local self-intersections and introduced the characteristic map defined by the subdominant eigenvectors. Moreover, for all stationary subdivision schemes he derived necessary and sufficient conditions which guarantee that the limiting surface is regular, i.e. tangent plane continuous without local penetrations.

Finally, in [8] Reif's characteristic map is used to parametrize the subdivision surface. With this parametrization it is possible to extent Reif's result and to obtain for all stationary subdivision schemes necessary and sufficient conditions which guarantee that the limiting surface is a regular G^k-surface.

Doo and Sabin [4], Ball and Storry [2] and Loop [7] used the smoothness criteria to find among certain variations of the Catmull/Clark and Loop's algorithm the best. However, these best algorithms still produce curvature discontinuous surfaces, see e.g. [2].

In [10] we took a different approach. Instead of varying the subdivision rules within some bounds which are set heuristically, we changed the spectrum of the subdivision matrix so as to obtain the desired properties. Using the G^2-characterization in [8] we derived a G^2-subdivision algorithm from the Catmull/Clark algorithm (which does not produce infinite curvatures), see [10].

Here we provide similar improvements, a G^1- and a G^2-algorithm based on the butterfly and Loop's algorithm.

2. Loop's algorithm

Loop's algorithm generalizes the subdivision algorithm for surfaces expressed in terms of the symmetric quartic box spline over a regular triangulation of $\mathbb{R}^2$. It generates from any triangular net $\mathcal{N}_0$ a new net $\mathcal{N}_1$, whose vertices are classified as E- and V-vertices.

Computing the weighted averages of the four vertices of any two triangles in $\mathcal{N}_0$ sharing a common edge with the weights shown in Figure 1 gives the E-vertices. Similarly computing the weighted averages of all vertices of all triangles in $\mathcal{N}_0$ around any vertex with the weights shown in Figure 1 gives the V-vertices. For $n = 6$ Loop chooses $\alpha(6) = 5/8$ since this corresponds to box spline subdivision.

The new net $\mathcal{N}_1$ is obtained by connecting for all triangles of $\mathcal{N}_0$ the associated three E-vertices and for all edges of $\mathcal{N}_0$ the associated E-vertices with both associated V-vertices. By the same procedure a next net $\mathcal{N}_2$ is obtained from $\mathcal{N}_1$ and so on.

[1] Supported by DFG grant # PR 565/1-1

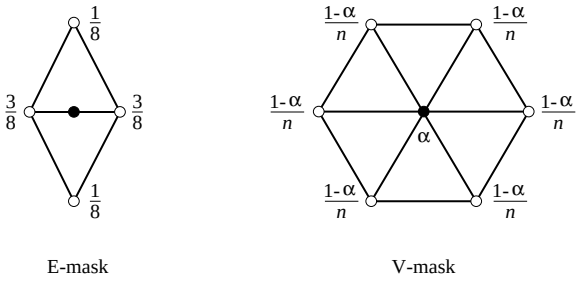

Figure 1. The masks of the Loop algorithm – the V-mask is illustrated for $n = 6$.

Note that a vertex of any net $\mathcal{N}_i, i \geq 1,$ is *extraordinary*, i.e. an interior vertex with valence $\neq 6$, if it is a V-vertex associated with an extraordinary vertex of $\mathcal{N}_{i-1}$. Thus the number of extraordinary vertices is constant for all nets $\mathcal{N}_i, i \geq 0,$ and these vertices are separated by more and more ordinary vertices as i grows.

In particular if $\mathcal{N}_0$ is a regular triangular net, i.e. without extraordinary vertices, Loop's algorithm coincides with the subdivision algorithm for quartic box spline surfaces. Thus also for an arbitrary net $\mathcal{N}_0$ the sequence $\mathcal{N}_i$ converges to a piecewise quartic surface with one extraordinary point for each extraordinary vertex of $\mathcal{N}_0$. The limiting surface is a C^2-surface everywhere except at its extraordinary points.

Loop's analysis shows that the limiting surface has a continuous tangent plane at its extraordinary points for a certain range of α's, see [7] .

3. The butterfly algorithm

The butterfly algorithm of Dyn et al. [5] generates a sequence of triangular nets $\mathcal{N}_i, i \geq 0,$ similar to Loop's algorithm. Only the masks used to compute the E- and V-vertices are different. They are given in Figure 2.

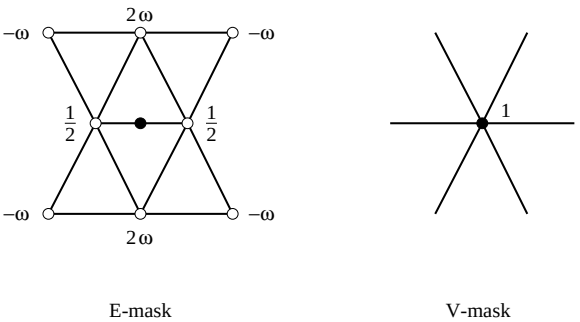

Figure 2. The masks of the butterfly algorithm.

A sequence of nets $\mathcal{N}_i$ obtained by the butterfly algorithm with small positive ω converges to a surface that is differentiable everywhere except at its extraordinary points of valence 3 [5, 6] and $n \geq 8$.

At extraordinary points of valence $n \geq 8$ the surface is tangent plane continuous but it has self-intersections and therefore is not regular. We checked this for several ω. However, in the sequel we always work with $\omega = 1/32$.

Variations of the butterfly algorithm have been proposed by Zorin et al. [16]. However, the smoothness of the limiting surfaces obtained by these variations has not yet been investigated.

4. A smoothness condition

In Sections 5 and 6 we present modifications of Loop's and the butterfly algorithm giving G^2- or G^1-surfaces in the limit. The method used to derive these modifications is based on the G^k-analysis of subdivision schemes given in [8] and can also be used for subdivision schemes for quadrilateral nets [10].

For more details we need to recall a result from [8]. We present it in the theorem below for any *subdivision scheme* $\mathcal{S}$ that is identical with the butterfly or Loop's algorithm except that E- and V-masks may be different.

We assume that the limiting surface associated with any initial triangular net $\mathcal{N}_0$ obtained by the subdivision scheme $\mathcal{S}$ has C^k-parametrizations around all its ordinary points.

Extraordinary points are isolated as observed in Section 2. Therefore, to analyze the smoothness of the limiting surface at extraordinary points it suffices to consider a subnet $\mathcal{M}_0$ of $\mathcal{N}_0$ consisting of one extraordinary vertex surrounded by say r_0 rings of ordinary vertices as illustrated in Figure 3 for $r_0 = 3$.

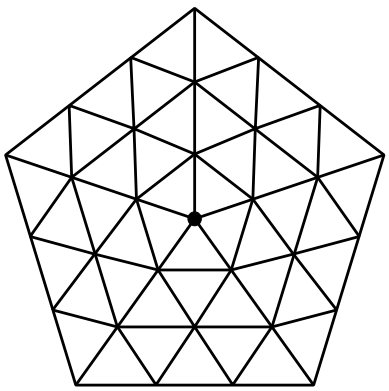

Figure 3. A net with one extraordinary vertex of valence 5 (marked by •) surrounded by $r_0 = 3$ rings of ordinary vertices.

Further let $\mathcal{M}_1$ be the largest subnet of $\mathcal{N}_1$ whose vertices depend only on $\mathcal{M}_0$. This net $\mathcal{M}_1$ also has only one extraordinary vertex surrounded by say r_1 rings of ordinary vertices.

Note that r_1 is roughly twice as lage as r_0. For example in Loop's algorithm $r_1 = 5$ if $r_0 = 3$ and in the butterfly algorithm $r_1 = 6$ if $r_0 = 4$.

Let r_0 be so large that $r_1 - r_0 \geq 1$. Then discarding the $r_1 - r_0$ outer rings of $\mathcal{M}_1$ gives a net $\mathcal{K}_1$ with the same size and connectedness as $\mathcal{M}_0$. Let $\mathbf{m}_1, \ldots, \mathbf{m}_m$ and $\mathbf{k}_1, \ldots, \mathbf{k}_m$ denote the vertices of $\mathcal{M}_0$ and $\mathcal{K}_1$, respectively. Since the vertices $\mathbf{k}_i$ are affine combinations of the $\mathbf{m}_j$, there is an $m \times m$ matrix A such that

$$[\mathbf{k}_1 \ \ldots \ \mathbf{k}_m]^t = A[\mathbf{m}_1 \ \ldots \ \mathbf{m}_m]^t.$$

Let $\mathbf{s}_0$ denote the limiting surface associated with $\mathcal{M}_0$ under the subdivision scheme $\mathcal{S}$. Applying $\mathcal{S}$ to $\mathcal{M}_1$ gives the same limiting surface $\mathbf{s}_0$, but the surface $\mathbf{s}_1$ associated with the subnet $\mathcal{K}_1$ is smaller and only a part of $\mathbf{s}_0$. Taking $\mathbf{s}_1$ away from $\mathbf{s}_0$ gives the here so-called *first surface ring associated with* $\mathcal{M}_0$.

Now we are able to present the following theorem which is proven in more general form in [8]:

Theorem 4.1 *Let A have the m (possibly complex) eigenvalues $1, \lambda, \lambda, \mu, \ldots, \zeta$, where $1 > |\lambda| \geq |\mu| \geq \ldots \geq |\zeta|$ and assume two eigenvectors $\mathbf{c}$ and $\mathbf{d}$ associated with the double eigenvalue λ. If the first surface ring of the net given by $[\mathbf{c}_1 \ldots \mathbf{c}_m]^t = [\mathbf{c}\ \mathbf{d}]$ is regular without self-intersections and*

$$|\lambda|^k > |\mu|, \quad k \geq 1, \tag{4.1}$$

then the limiting surface is a G^k-surface for almost all initial nets $\mathcal{M}_0$. (More precisely, the limiting surface is a G^k-surface for all initial nets $\mathcal{M}_0$ whose expansion by the eigenvectors of A involves $\mathbf{c}$ in one and $\mathbf{d}$ in a second coordinate.)

The eigenvalue condition (4.1) goes back to Doo and Sabin [4]. The first surface ring associated with the eigenvectors $\mathbf{c}$ and $\mathbf{d}$ is called the *characteristic map of* A by Reif who used it to prove this Theorem for $k = 1$ [11].

If the limiting surface in Theorem 4.1 is a C^k-manifold, $k \geq 2$, then the extraordinary point is a flat point. This fact is also true for more general subdivision schemes, see [11, 9].

5. Modifications of Loop's algorithm

The subdivision matrix A of Loop's algorithm associated with an extraordinary vertex of valence n has a single dominant eigenvalue 1 and satisfies the G^1-conditions of Theorem 4.1 [7, 15], but not the G^2-condition [14]. To obtain a subdivision matrix A' that represents a modification of Loop's algorithm satisfying the G^2-condition we diagonalize the matrix A,

$$A = V \Lambda V^{-1}, \quad \text{where } \Lambda = \text{diag}(1, \lambda, \lambda, \mu, \ldots, \zeta),$$

change the modal matrix Λ to

$$\Lambda' = \text{diag}(1, \lambda, \lambda, \mu', \ldots, \zeta'), \quad \text{where } |\mu'|, \ldots, |\zeta'| < \lambda^2,$$

and compute the new subdivision matrix as

$$A' = V \Lambda' V^{-1}.$$

Lemma 5.1 *The matrices A and A' have the same characteristic maps.*

Proof The eigenvectors associated with λ are the same for A and A'. They define a planar control net $\mathcal{N}_0$. Subdividing $\mathcal{N}_0$ by Loop's algorithm and also by the modification results both times in the same sequence of nets $\mathcal{N}_i$. The extraordinary vertex and its three surrounding rings of control points in $\mathcal{N}_i$ are scaled versions of $\mathcal{N}_0$. The other control points of $\mathcal{N}_i$ are computed by the subdivision rules for regular nets. Thus Loop's algorithm and its modification applied to $\mathcal{N}_0$ produce the same surface in the limit. □

The symmetry of Loop's scheme means that the subdivision matrix A is block-circulant. Therefore a discrete Fourier transformation can be used to analyze the spectral properties of A.

If $n = 3$, the matrix A has the subdominant eigenvalue $\lambda = 1/4$ and exactly six eigenvalues with modulus in the half-open interval $[|\lambda|^2, |\lambda|)$. These are the two triple eigenvalues $1/8$ and $1/16$. Changing just these triple eigenvalues to the triple eigenvalues $1/8 + \varepsilon_1$ and $1/16 + \varepsilon_2$, respectively, such that $1/8 + \varepsilon_1$ and $1/16 + \varepsilon_2$ are less than $|\lambda|^2$, results in a matrix A', which represents the same masks as the original matrix A except for the E- and V-masks shown in Figure 4, where

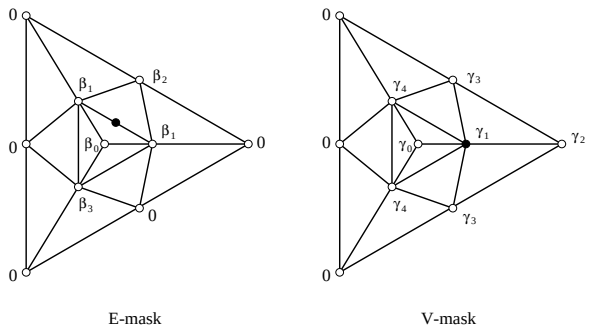

E-mask V-mask

Figure 4. The E- and V-masks of the modified Loop algorithm near a vertex of valence $n = 3$.

$$
\begin{aligned}
\beta_0 &= \tfrac{1}{8} - \tfrac{\varepsilon_1}{2(2\alpha-1)},\\
\beta_1 &= \tfrac{3}{8} + \tfrac{(16\alpha-7)\varepsilon_1}{6(2\alpha-1)},\\
\beta_2 &= \tfrac{1}{8} - \varepsilon_1,\\
\beta_3 &= -\tfrac{(20\alpha-11)\varepsilon_1}{6(2\alpha-1)},\\
\gamma_0 &= \tfrac{1}{16} - \tfrac{\varepsilon_1}{2\alpha-1} + \tfrac{3\varepsilon_2}{16\alpha-7},\\
\gamma_1 &= \tfrac{5}{8} + \tfrac{(20\alpha-11)\varepsilon_1}{3(2\alpha-1)} + \tfrac{(16\alpha-10)\varepsilon_2}{3(16\alpha-7)},\\
\gamma_2 &= \tfrac{1}{16} - \varepsilon_2,\\
\gamma_3 &= \tfrac{1}{16} - \varepsilon_1 + \varepsilon_2,\\
\gamma_4 &= \tfrac{1}{16} - \tfrac{(2\alpha-2)\varepsilon_1}{3(2\alpha-1)} - \tfrac{(32\alpha-11)\varepsilon_2}{3(16\alpha-7)}.
\end{aligned}
$$

If $n \geq 4$, the matrix A has $k := \lfloor (n-1)/2 \rfloor - 1$ double eigenvalues besides λ. We denote these eigenvalues by $\mu_1, \ldots, \mu_k$ and assume $|\mu_1| \geq \ldots \geq |\mu_k|$. Furthermore, any eigenvalue of A with modulus in the half-open interval $[|\lambda|^2, |\lambda|)$ is one of these double eigenvalues μ_i but not vice versa.

Changing just these double eigenvalues μ_i to the double eigenvalues $\mu_i + \delta_i$ results in a matrix A', which represents the same masks as the original matrix except for the E-mask illustrated in Figure 5, where

$$
\alpha_i = f_i + \frac{2}{n} \sum_{j=1}^{k} \delta_j \cos\left(\frac{2\pi i (j+1)}{n} \right), \; i = 0, \ldots, \lfloor n/2 \rfloor \tag{5.2}
$$

and

$$
f_i = \begin{cases} 3/8 & i = 0 \\ 1/8 & \text{if } i = 1 \\ 0 & i \geq 2 \end{cases}.
$$

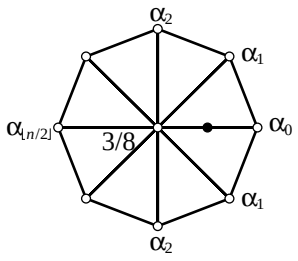

Figure 5. The E-masks of the modified Loop algorithm near the vertices of valence $n \geq 4$ illustrated for $n = 8$.

Note that Loop's masks, see Figure 1, are obtained if all δ's and ε's are zero.

Figure 6 shows an example. The surface at the top is generated using Loop's algorithm while the one at the bottom is produced with the above modified masks, where $\delta_1 = 0.03755$ and $\delta_2 = \ldots, \delta_k = 0$. The surfaces are shown with the visualization of their Gaussian curvature. This curvature is not a discrete approximation obtained from the subdivided control net. We used the piecewise quartic parametrization of the surface to compute the Gaussian curvature. The common control net of both surfaces is given in Figure 7.

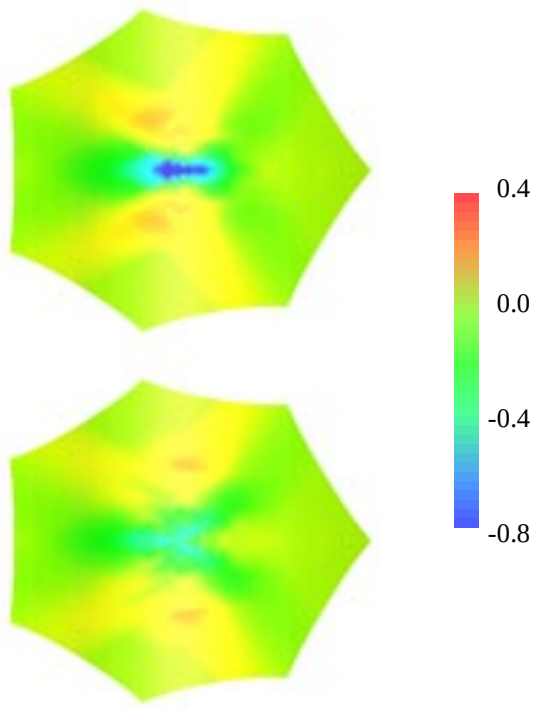

Figure 6. Visualization of the Gaussian curvature of the surface generated from the net shown in Figure 7 by Loop's algorithm (top) and our modification (bottom).

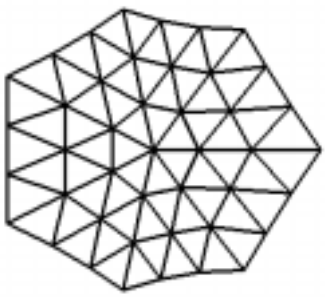

Figure 7. Topview of the control net used for Figure 6. It lies on a parabolic cylinder.

Remark 5.2 *The eigenvalues of A with modulus less than $|\lambda|^2$ need not be changed. However, the masks of the modified algorithms have negative weights, see (5.2). Therefore the eigenvalues with modulus $< \lambda^2$ can be changed so as to obtain larger negative weights.*

Remark 5.3 *In some cases better looking surfaces are obtained if Loop's algorithm is gradually modified after each subdivision iteration. For example, the sequence of nets $\mathcal{N}_i, i = 0, \ldots, 6$, leading to the surface shown in Figure 8 (bottom left) has been obtained by Loop's algorithm modified with $\varepsilon_1 = 2\varepsilon_2 = \sqrt{i/384}$ when applied to the net $\mathcal{N}_i$. The adaptive linear combination of Loop's and our scheme produces a surface with a more even curvature distribution and without infinite curvature.*

In further iterations we would chose ε_1 and ε_2 constant as in step 6. Note that the modified subdivision matrix satisfies the conditions of Theorem 4.1 for $i \geq 2$.

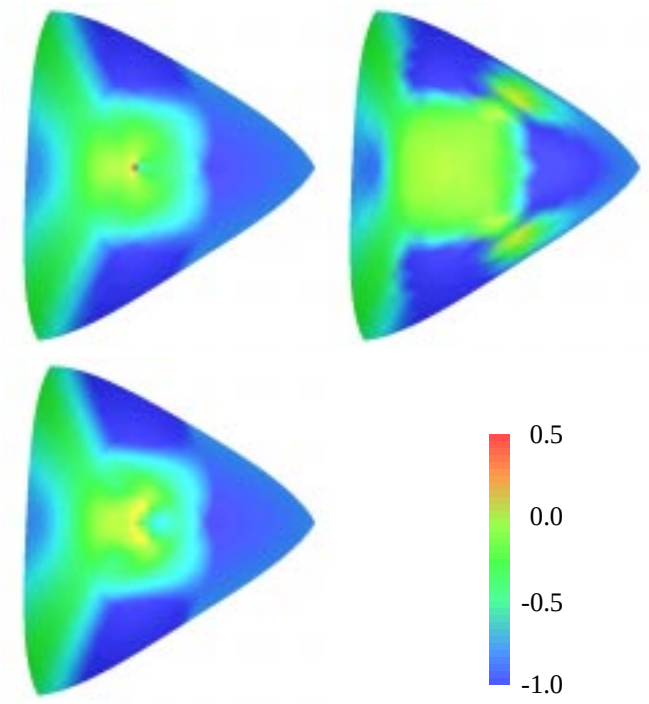

Figure 8. Visualization of the Gaussian curvature of the surface generated from the net shown in Figure 9 by Loop's algorithm (top left), our modified scheme (top right) and an adaptive linear combination of Loop's and our scheme (bottom left).

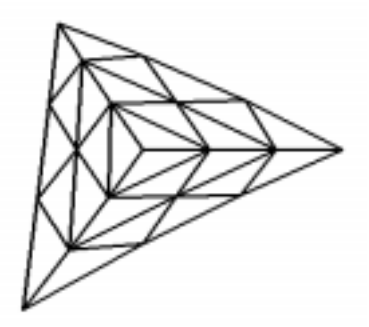

Figure 9. Topview of the control net used for Figure 8. It lies on a hyperbolic paraboloid.

6. Modifications of the butterfly algorithm

A limiting surface obtained by the butterfly algorithm is not differentiable at extraordinary points, in general.

For an extraordinary point of valence 3, this is due to the fact that the associated subdivision matrix A has a triple subdominant eigenvalue λ, see [5]. Two of these eigenvalues are associated with eigenvectors forming a regular injective characteristic map. As in Section 5 we change the third eigenvalue λ to $\lambda - 0.01$.

For an extraordinary point of valence $n \geq 8$ the characteristic map of the subdivision matrix A overlaps itself. Since the matrices are block circulant they have a discrete Fourier transform, which helps to understand what happens: The subdominant eigenvalues for $n \geq 8$ correspond to higher frequencies than one. Luckily both eigenvectors associated with the largest eigenvalue of frequency one (it is a double real eigenvalue, here denoted by ν) represent the control net of a regular injective surface ring.

Thus we change the eigenvalues with modulus in $(1, |\nu|)$ to $\nu - 0.01$ as in Section 5 so that ν becomes the subdominant eigenvalue.

Together these changes lead to a modification of the butterfly algorithm for $\omega = 1/32$ which is presented by the same masks except for the masks given in Figure 11, where the weights $\alpha_i, \beta_i, \gamma_i$ are given in Table 10.

Figure 12 shows an example. The surface at the top is generated using the butterfly scheme while the one at the bottom is produced with the above modified masks. Note that the surface at the top has self-intersections while the surface at the bottom as well as the common control net of both surfaces, see Figure 13, have no self-intersections.

Remark 6.1 *The surface obtained by the modified butterfly algorithm does not interpolate all vertices of the initial control net. However, if we use the butterfly algorithm in the first iteration and the modification in all further iterations, all vertices of the initial net are interpolated.*

$n=3$			$n=8$		
$\alpha_0,\ldots,\alpha_6$	$\beta_0,\ldots,\beta_6$	$\gamma_0,\ldots,\gamma_6$	$\alpha_0,\ldots,\alpha_{14}$	$\beta_0,\ldots,\beta_{14}$	$\gamma_0,\ldots,\gamma_{13}$
			0.500000	0.000000	0.062500
			0.493006	0.985866	0.063594
			−0.000063	−0.000129	0.492427
			−0.030744	0.001021	−0.031319
0.512437	0.029142	0.089508	0.062500	0.000000	0.000000
0.495142	0.988619	0.064309	0.000000	0.000000	−0.023677
−0.000122	−0.000285	0.489452	−0.000505	−0.001021	0.000069
−0.030416	0.001952	−0.031515	−0.024256	0.014133	−0.001094
0.026392	−0.011380	0.001809	0.000063	0.000129	0.007572
−0.000122	−0.000285	−0.073047	−0.000505	−0.001021	0.000069
0.000833	0.001952	−0.000265	0.000000	0.000000	0.000000
			0.000000	0.000000	−0.007572
			0.000505	0.001021	−0.000069
			−0.006993	−0.014133	0.001094
			−0.000063	−0.000129	

$n=9$			$n=10$		
$\alpha_0,\ldots,\alpha_{15}$	$\beta_0,\ldots,\beta_{15}$	$\gamma_0,\ldots,\gamma_{15}$	$\alpha_0,\ldots,\alpha_{17}$	$\beta_0,\ldots,\beta_{17}$	$\gamma_0,\ldots,\gamma_{16}$
			0.500000	0.000000	0.062500
0.500000	0.000000	0.062500	0.487959	0.976213	0.064752
0.489067	0.978322	0.064383	−0.000137	−0.000270	0.484007
−0.000112	−0.000223	0.486686	−0.030139	0.002193	−0.031432
−0.030342	0.001799	−0.031386	0.058779	−0.007350	0.000696
0.060601	−0.003764	0.000327	−0.000042	−0.000083	−0.025141
−0.000019	−0.000038	−0.022560	−0.000424	−0.000837	0.000069
−0.000592	−0.001174	0.000089	−0.021509	0.019243	−0.001822
−0.020976	0.020370	−0.001769	0.000110	0.000219	0.019767
0.000105	0.000209	0.016331	−0.001372	−0.002710	0.000225
−0.001113	−0.002207	0.000168	0.009740	0.019243	−0.001822
0.005466	0.010838	−0.000941	0.000110	0.000219	0.006108
0.000056	0.000111	−0.003017	−0.000424	−0.000837	0.000069
0.000205	0.000407	−0.000031	−0.003720	−0.007350	0.000696
−0.008374	−0.016606	0.001442	−0.000042	−0.000083	−0.015992
−0.000086	−0.000170	−0.017379	0.001110	0.002193	−0.000182
0.001184	0.002349	−0.000178	−0.012040	−0.023786	0.002252
			−0.000137	−0.000270	

$n=11$			$n=12$		
$\alpha_0,\ldots,\alpha_{18}$	$\beta_0,\ldots,\beta_{18}$	$\gamma_0,\ldots,\gamma_{18}$	$\alpha_0,\ldots,\alpha_{20}$	$\beta_0,\ldots,\beta_{20}$	$\gamma_0,\ldots,\gamma_{19}$
			0.500000	0.000000	0.062500
0.500000	0.000000	0.062500	0.479428	0.958659	0.066361
0.488152	0.976494	0.064883	−0.000235	−0.000472	0.473093
−0.000147	−0.000291	0.483163	−0.029375	0.003762	−0.031566
−0.030063	0.002354	−0.031459	0.056948	−0.011103	0.001189
0.057578	−0.009764	0.000989	−0.000074	−0.000148	−0.020999
−0.000061	−0.000121	−0.028401	−0.000684	−0.001382	0.000093
−0.000200	−0.000398	0.000035	−0.016230	0.030236	−0.002671
−0.023491	0.015393	−0.001560	0.000160	0.000323	0.026906
0.000096	0.000191	0.019202	−0.001874	−0.003762	0.000316
−0.001353	−0.002685	0.000238	0.011103	0.022207	−0.002379
0.011368	0.022553	−0.002286	0.000148	0.000297	0.006405
0.000141	0.000280	0.013105	−0.000505	−0.000996	0.000129
−0.000923	−0.001832	0.000162	−0.003915	−0.008028	0.000292
0.001686	0.003345	−0.000339	−0.000012	−0.000025	−0.010250
0.000020	0.000041	−0.008313	0.000684	0.001382	−0.000093
0.000586	0.001162	−0.000103	−0.005551	−0.011103	0.001189
−0.009967	−0.019774	0.002004	−0.000074	−0.000148	−0.006405
−0.000123	−0.000245	−0.020013	0.000505	0.000996	−0.000129
0.001410	0.002799	−0.000248	−0.001636	−0.003075	0.000897
			−0.000062	−0.000122	

Table 10. The weights of the masks of the modified butterfly algorithm for $n = 3$ and $n = 8, \ldots, 12$.

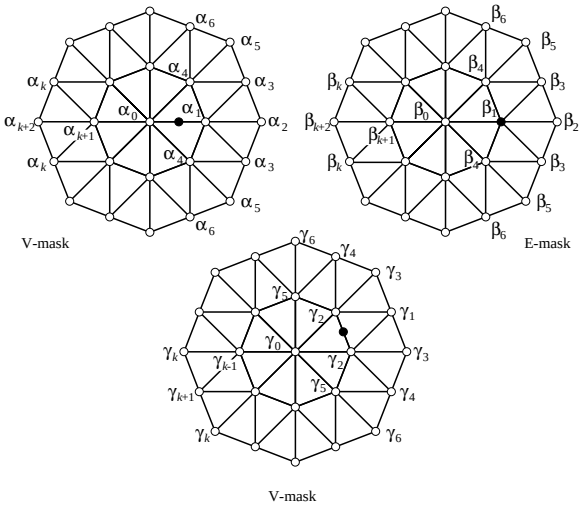

Figure 11. The E- and V-masks of the modified butterfly algorithm near a vertex of valence $n = 8$.

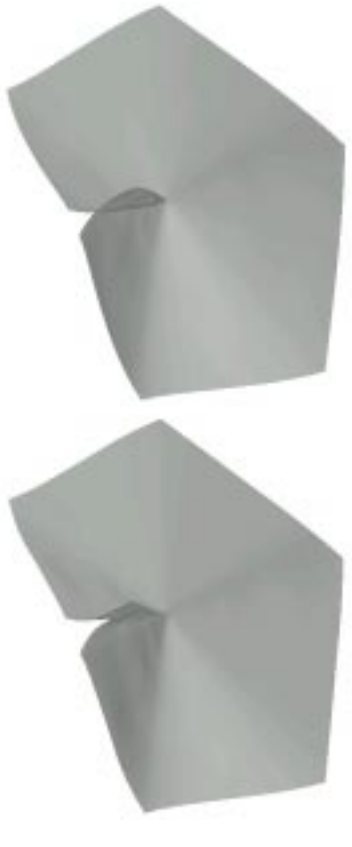

Figure 12. The surface generated from the net shown in Figure 13 by the butterfly scheme (top) and our modification (bottom).

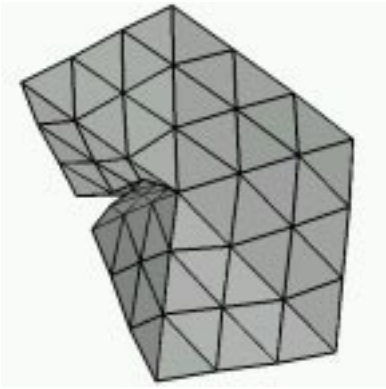

Figure 13. The control net used for Figure 12.

7. Acknowledgements

We wish to thank Uwe Klotz who helped us to generate Figures 6, 8 and 12.

References

[1] A. Ball and D. Storry. A matrix approach to the analysis of recursively generated B–spline surfaces. *Computer Aided–Design*, 18(8):437–442, 1986.

[2] A. Ball and D. Storry. Conditions for Tangent Plane Continuity over Recursiveley Generated B–spline Surfaces. *ACM Transactions on Graphics*, 7(2):83–102, 1988.

[3] E. Catmull and J. Clark. Recursive generated B–spline surfaces on arbitrary topological meshes. *Computer Aided–Design*, 10(6):350–355, 1978.

[4] D. Doo and M. Sabin. Behaviour of recursive division surfaces near extraordinary points. *Computer Aided–Design*, 10(6):356–360, 1978.

[5] N. Dyn, J. Gregory, and D. Levin. A Butterfly Subdivision Scheme for Surface Interpolation with Tension Control. *ACM Transactions on Graphics*, 9(2):160–169, 1990.

[6] N. Dyn, D. Levin, and C. Micchelli. Using parameters to increase smoothness of curves and surfaces generated by subdivision. *Computer Aided Geometric Design*, 7:129–140, 1990.

[7] C. Loop. Smooth Subdivision Surfaces Based on Triangles. Master's thesis, Department of Mathematics, University of Utah, Aug. 1987.

[8] H. Prautzsch. Analysis of C^k–subdivision surfaces at extraordinary points. Preprint 04/98, Fakultät für Informatik, Universität Karlsruhe, 1998. `http://i33www.ira.uka.de`.

[9] H. Prautzsch and U. Reif. Necessary Conditions for Subdivision Surfaces. Sonderforschungsbereich 404, Universität Stuttgart, Bericht 97/04, 1997.

[10] H. Prautzsch and G. Umlauf. A G^2-subdivision algorithm. To appear in: Bieri, Brunnet, Farin, editors, *Proceedings of the Dagstuhl conference on geometric modelling 1996*, Computing suppl., 1998.

[11] U. Reif. A unified approach to subdivision algorithms near extraordinary vertices. *Computer Aided Geometric Design*, 12:153–174, 1995.

[12] U. Reif. A Degree Estimate for Subdivision Surfaces of Higher Regularity. *Proceedings of the American Mathematical Society*, 124(7):2167–2174, 1996.

[13] M. Sabin. Cubic Recursive Division With Bounded Curvature. In P. Laurent, A. L. Méhauté, and L. Schumaker, editors, *Curves and Surfaces*, pages 411–414. Academic Press, Boston, 1991.

[14] G. Umlauf. Verbesserung der Glattheitsordnung von Unterteilungsalgorithmen für Flächen beliebiger Topologie. Master's thesis, IBDS, Universität Karlsruhe, Apr. 1996.

[15] G. Umlauf. Analyzing the characteristic map of triangular subdivision schemes. Preprint, IBDS, Universität Karlsruhe, 1998. In preparation.

[16] D. Zorin, P. Schröder, and W. Sweldens. Interpolatory Subdivision for Meshes with Arbitrary Topology. *Computer Graphics (ACM SIGGRAPH '96 Proceedings)*, pages 189–192, 1996.